University of California Transportation Center
UCTC-FR-2010-18

On the capacity of isolated, curbside bus stops

Weihua Gu, Yuwei Li,
Michael J. Cassidy, and Julia B. Griswold
University of California, Berkeley
August 2010

On the capacity of isolated, curbside bus stops

Weihua Gu *, Yuwei Li, Michael J. Cassidy, Julia B. Griswold

416 Mclaughlin Hall, Department of Civil and Environmental Engineering, University of California, Berkeley, CA 94720, United States

Abstract

The maximal rates that buses can discharge from bus stops are examined. Models were developed to estimate these capacities for curbside stops that are isolated from the effects of traffic signals. The estimates account for key features of the stops, including their target service levels assigned to them by a transit agency. Among other things, the models predict that adding bus berths to a stop can sometimes return disproportionally high gains in capacity. This and other of our findings are at odds with information furnished in professional handbooks.

Keywords: bus stop capacity; bus stop queueing

1 Introduction

While serving passengers at a busy stop, buses can interact in ways that limit their discharge flows. This can degrade the bus system's overall service quality (Fernandez and Planzer, 2002; Gibson et al., 1989).

The present paper explores the bus discharge flows that can be achieved at stops where buses dwell curbside to load and unload passengers. We will examine stops that are isolated from the influences of traffic signals and other bus stops; where sufficient space exists for storing the bus queues that can form immediately upstream of the stops; where bus movements in and around the stops are not affected by other (e.g. car) traffic; and where bus overtaking maneuvers are prohibited, both within any bus queues immediately upstream, and at the stops themselves, should multiple berths (i.e. bus loading areas) exist there.[1]

The rates that buses can discharge from stops of this kind depend in part on the target service level chosen by the transit agency. In this paper, we use a metric of service level called the failure rate, FR , defined as the probability that a bus arriving to a stop is temporarily blocked from using it by another bus. Though other service metrics (e.g. average bus wait time) are possible, FR is the metric featured in professional handbooks (e.g. TRB 2000 and 2003). Intuitively, the

* Corresponding author. Tel.: +1 (510) 931-6646; fax: +1 (510) 643-8919.
E-mail address: weihuagu@berkeley.edu.

[1] Cities often enact this prohibition because an overtaking bus can disrupt car traffic in the adjacent lane(s).

bus discharge flow increases as FR increases, and is highest when a bus queue is always present at the stop's entrance, i.e. when $FR = 1$.[2]

In light of this influence, we shall define bus-stop capacity as the maximal rate that buses can discharge from a stop for a specified threshold of FR . This definition is common in the literature (see again TRB 2000 and 2003). Our findings, on the other hand, are largely at odds with earlier publications, as we shall see. We shall arrive at these findings by developing (and evaluating) models that predict bus-stop capacities as functions of not only FR , but also bus arrival process and bus service time distribution.

A review of earlier work is furnished in the following section. Present findings in regard to stops with only one berth are provided in Section 3. Findings on multi-berth stops are in Section 4. Practical implications are discussed in Section 5.

2 Literature Review

The *Highway Capacity Manual* (TRB, 2000) reports that the capacity of a single-berth stop is inversely proportional to the sum of i) the bus' average service time; and ii) a second term that accounts for both the variation in this service time and the FR .[3] With this latter term, a stop's capacity increases with increasing FR , but only to a point. Curiously, the formula in the *Highway Capacity Manual* (henceforth *HCM*) predicts that capacity is maximal when FR reaches 0.5. Intuition, on the other hand, tells us that single-berth capacity is maximal when a bus queue always persists upstream; i.e., when FR is 1. Of further concern, the current edition of the *HCM* omits any discussion on the influence of the bus arrival process on stop capacity.[4]

For a multi-berth stop, the *HCM* takes capacity to be the product of the single-berth capacity and the number of "effective" berths. The *HCM* furnishes values for this latter term that result in steadily diminishing returns to capacity, meaning that each new berth that is added to a stop will return less than a proportional increase in the stop's capacity (see Table 27-12 of the TRB 2000). Presumably, this is to account for the disruptive bus interactions that can occur at multi-berth stops (see our discussion of the "blocking effect" in Section 4.1). However, the inefficiencies brought with each added berth are assumed in the *HCM* to be independent of all other factors, including: FR , bus arrival process, and service time variation.

---

[2] If buses were controlled so that their arrival headways and service time at a stop were perfectly coordinated, the stop could, in theory, always be occupied without queues forming. The FR in this idealized (and unrealistic) case would therefore be zero, though the bus discharge flow would be high.

[3] The second term involves both: the one-tail standard normal variate corresponding to FR ; and the coefficient of variation of bus service time (see Equation 27-5 of TRB, 2000).

[4] Although an earlier edition of the *HCM* includes a multiplicative adjustment factor that reportedly accounts for variations in bus arrival headway, the factor seems instead to account for FR (see Equation 12-7 and Table 12-17 of TRB, 1985).

Much of the above is at odds with our present findings (see Sections 3 and 4). What thus appear to be shortcomings of the *HCM* take on greater significance because they are repeated in the *Transit Capacity & Quality of Service Manual* (TRB, 2003). This latter handbook will reportedly supplant discussion of transit systems in future editions of the *HCM*. The same ideas, moreover, have found their way into the *Transportation Planning Handbook* (ITE, 1999).

Critiques of these capacity formulas already appear in the literature. Gibson et al. (1989), for example, argues that the complex stochastic processes at real bus stops limit the usefulness of *HCM* formulas. Fernandez and Planzer (2002) reports that the formulas tend to under-predict field-measured estimates of stop capacity. These findings are useful in that they highlight certain influences on bus-stop capacity. Yet, they do little to quantify these influences.

Similarly, studies to increase the capacity of a multi-berth stop by either dispatching buses in certain ways (Gardner et al., 1991; Szász et al., 1978), or by reconfiguring the stop's geometry (Gibson et al., 1989; St. Jacques and Levinson, 1997; etc.) offer only limited insights into cause and effect. The same is true of past efforts to estimate the parameter values for describing bus arrival processes (Danas, 1980; Fernandez, 2001; Ge, 2006; Kohler, 1991) and service time distributions (Ge, 2006; St. Jacques and Levinson, 1997).

3 Single-Berth Stops

It will be assumed that bus stops operate in the steady-state, such that the arrival process and the service time distribution are both time-invariant, and that the long-run average bus arrival rate never exceeds the stop's capacity when FR is 1. In this steady-state, the average bus inflow to the stop always equals the average outflow.

Although some empirical studies show that bus arrivals at stops follow a Poisson process (Danas, 1980; Ge, 2006; Kohler, 1991), other studies (e.g. Fernandez, 2001) argue that this is not always the case. To simplify our analysis and highlight the findings, we start by assuming two special cases in regard to the bus arrival process: Poisson arrivals (in Section 3.1), as can occur when the stop serves multiple bus routes; and uniform bus arrivals (in Section 3.2), as may occur, at least in theory, when the stop serves a single route with buses that are rigidly controlled. Finally, Section 3.3 examines the case of a more general bus arrival pattern. Capacity formulas will be furnished for each of these three cases.

3.1 Poisson Bus Arrivals

In the steady-state, Poisson bus arrivals to a stop satisfy the PASTA (Poisson Arrivals See Time Averages) property; see Gross, et al. (2008). This implies that FR is equal to the fraction of time that the stop's single berth is utilized. This utilization fraction is the ratio of bus inflow, λ, to the single-berth stop's maximal service rate (i.e. the inverse of the average time that each bus spends serving passenger boarding and alighting movements). We denote this maximal service rate as μ. Thus, for $\lambda < \mu$,

$$\frac{\lambda}{\mu} = FR \quad . \tag{1}$$

Since λ can be viewed equivalently as the stop's capacity for a specified FR; and since μ is the stop's output flow when $FR = 1$; the ratio $\frac{\lambda}{\mu}$ will henceforth be termed the normalized capacity.

As per intuition, (1) shows that single-berth capacity is maximal when $FR = 1$. It further shows that for Poisson bus arrivals, capacity is independent of the variation in bus service time (for boarding and alighting movements). This independence turns out not to hold in general, however, as we shall see next.

3.2 Uniform Bus Arrivals

Assume now that the bus arrival headways are deterministic and equal. Further assume that bus service time follows an Erlang-k distribution, which is a more general distribution than the commonly-used exponential distribution (and has been observed in Ge, 2006 to be suitable at some stops.) For this present case, our model does not have a closed-form solution. An analytical model that can be solved numerically is derived in Appendix A. A simple, closed-form approximation to the solution of this model is found to be:

$$\frac{\lambda}{\mu} = FR^{\frac{C_S}{1.001 + 0.26 C_S}} \quad , \tag{2}$$

where C_S is the coefficient of variation in bus service time.

Equation (2) came by fitting a curve to our numerical solutions over the range of $C_S \in [0, 1]$, since this is consistent with the range of C_S observed in the literature (St. Jacques and Levinson, 1997). The result satisfies intuitive boundary conditions for the relation between FR and $\frac{\lambda}{\mu}$.[5] The inclusion of C_S in (2) is logical, since $k = C_S^{-2}$ for Erlang distributions, and this shows how stop capacity for the case of uniform bus arrivals depends on the coefficient of variation in bus service time as well as on FR.

To explore matters more deeply, relations generated from (2) are shown with solid curves in Figure 1 for $C_S =$ 0.1, 0.5, and 1. These curves collectively reveal that, for uniform arrivals and for $0 < FR < 1$, capacity increases as the coefficient of variation in bus service time diminishes. The curves further show that the maximal capacity of the stop (when $FR = 1$) is the same for all C_S. The case of $C_S = 0$ corresponds to the perfect coordination of bus arrivals and bus service

[5] These conditions are: i) $\frac{\lambda}{\mu} = 0$ if $FR = 0$ and $C_S > 0$; and ii) $\frac{\lambda}{\mu} = 1$ if $FR = 1$ and if $C_S = FR = 0$.

time, as previously discussed in Footnote 2, such that $FR = 0$. The curve in this idealized case therefore reduces to a point, also as shown in Figure 1.

The relation for Poisson bus arrivals revealed in (1) is shown in Figure 1 as well; see the dashed line. Comparing this dashed line against the solid curves reveals that for $0 < FR < 1$, capacity also increases with diminishing variation in bus headways. (We can see this because the coefficient of variation is 0 and 1 for uniform and Poisson bus arrivals, respectively).

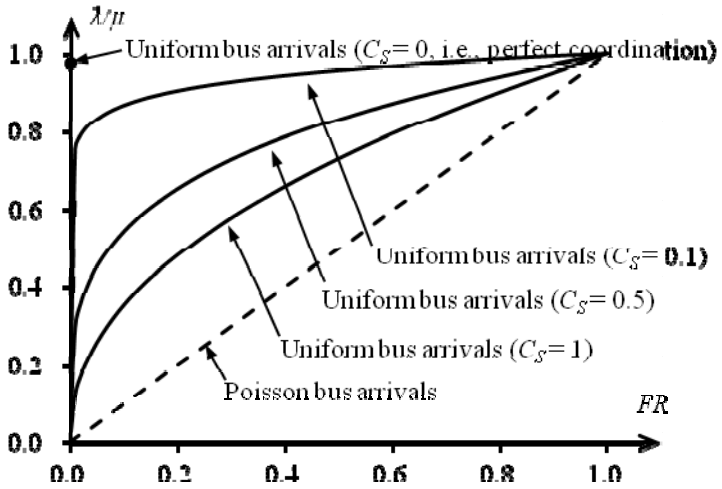

Figure 1 – Normalized capacity versus FR for single-berth stops; comparisons between Poisson and uniform bus arrivals

3.3 General Bus Arrivals

We continue to model bus service time as above, and now use the Erlang-i distribution to describe a more general distribution for bus headways. A numerical solution was derived in similar fashion to the uniform bus-arrival case, for which an approximation is found to be:

$$\frac{\lambda}{\mu} = FR^{\frac{0.42C_H^2 + 0.58C_S^2 - 0.29C_H^2 C_S^2}{1 - 0.58C_H^2 + 0.58C_S^2 - 0.29C_H^2 C_S^2}}, \quad (3)$$

where C_H is the coefficient of variation of bus arrival headways.

From (3) we see that stop capacity is influenced by service time and headway variations. Readers can verify that reductions in the coefficient of variation for either of these factors will increase a stop's capacity when $0 < FR < 1$, and $0 \leq C_H, C_S \leq 1$; e.g. one can fix either C_H or C_S and

obtain curves that are qualitatively similar (in their shapes and their relative positions) to the solid curves in Figure 1.[6]

4 Multi-Berth Stops

Two competing effects, which we term the "blocking" and the "berth pooling" effects, are found to influence the capacity of multi-berth stops, as explained in Section 4.1. The returns to capacity from added berths are studied for two limiting cases that isolate the above effects and for a third, more general case, all in Section 4.2. Further findings come by examining how returns to capacity are influenced by coefficients of variation in bus service time and bus headway, as shown in Section 4.3. For all these analyses, we will assume that the distribution of an individual bus' service time (to load and unload passengers) is independent of the stop's number of berths.

4.1 Two Competing Effects

Discussion begins with the blocking effect. A bus can enter a stop only when its upstream-most berth is open. (At this time, the entering bus proceeds as far as possible until encountering the end of the stop or a dwelling bus; and the entering bus will then dwell at the downstream-most available berth for its entire time in the stop.) Similarly, a bus can discharge from a stop only after all buses that were previously dwelling at that stop's downstream berths have departed. This blocking effect for entering and exiting a stop tends to diminish the stop's returns to capacity brought by added berths. The effect diminishes, however, when the load rate, R, approaches 0, where $R = \frac{\lambda}{c\mu}$ and c is the number of berths at the stop.

We illustrate the second effect, berth pooling, with the following example. Consider two independent, single-berth stops, each with equal bus arrival rate, λ, as shown on the left side of Figure 2. (Dashed boxes in this figure denote berths, and shaded rectangles denote buses). If we ignore the blocking effect, the fluctuations in bus arrivals would be better served by pooling the two berths into a single, double-berth stop, as shown on the right side of Figure 2. Thus for the same total bus arrival rate (2λ for both the left and right sides in the figure), this berth pooling effect means that the double-berth stop would enjoy a lower FR than would the two single-berth stops; i.e., the double-berth stop would have a higher capacity for a given FR. Berth pooling tends to improve the stop's returns to capacity brought by added berths. The effect diminishes, however, when R approaches its maximum, meaning when the input flow, λ, approaches the stop's maximal capacity (see Equation 4).

[6] In addition to satisfying the conditions in Footnote 5, Equation (3) reduces to (1) for the case of Poisson bus arrivals where $C_B = 1$. As an aside, analysis shows that (3) produces significantly lower capacities as compared with the formulas of the *HCM* (TRB, 2000).

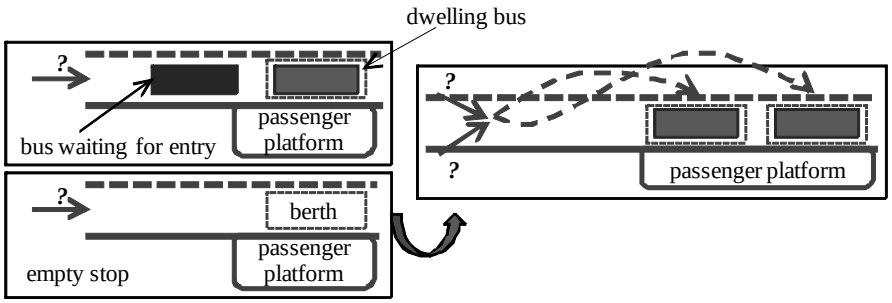

Figure 2 – Berth pooling effect

The above effects are countervailing: as R approaches 0 or its maximum, one effect diminishes while the other dominates.[7] We will therefore isolate the two effects by examining multi-berth stops under the two limiting cases for R .

4.2 Returns to Capacity

We next explore the returns to capacity i) when R is maximal; ii) when $R = 0$; and iii) for the general case when R falls between these limits.

4.2.1 Limiting case when R is maximal

In this case, queued buses enter a stop in platoons of size c , and the time required to serve a platoon is the maximal bus service time across the platoon. The stop's maximal capacity, $Q(c)$, is therefore:

$$Q(c) = \frac{c}{E[T(c)]} = \frac{c}{\int_{t=0}^{\infty}(1-(F_S(t))^c)dt} \quad (4)$$

where $E[T(c)]$ is the expected value of the platoon service time; and $F_S(t)$ is the cumulative distribution function of the individual bus service time. The derivation of (4) is furnished in Appendix B. Intuitively, the bus arrival pattern (to the rear of the queue) does not influence capacity in this limiting case.

The average capacity per berth, $\frac{1}{E[T(c)]}$, decreases with added berths, since $E[T(c)]$ increases with c . Thus from the first equality in (4), we see how the blocking effect can create decreasing returns to capacity.

[7] As per Footnote 2, an exception can occur under perfect coordination; i.e., when platoons of c buses arrive at uniform intervals and the service time is constant. In this case, neither blocking nor berth pooling take effect and the FR is always zero.

4.2.2 Limiting Case of $R \rightarrow 0$

Computer simulation is used next to explore stop capacity under this second limiting case. The logic of our simulation model is described in Appendix C. For the analysis to follow, bus service time is assumed to follow the gamma distribution (a generalization of the Erlang distribution) with $C_S = 0.6$, as recommended by St. Jacques and Levinson (1997). Bus arrivals are assumed to follow a Poisson process, as if the stop were used by multiple bus lines. Simulations of other bus arrival patterns and service time distributions yield qualitatively similar results.

The curves in Figure 3 display the normalized incremental change in stop capacity achieved for each added berth, $\frac{\Delta\lambda}{\mu}$, for the first through the sixth berth. These curves are shown for near-zero values of FR , since it is the assumed metric of interest and is a reasonable proxy for R . (Note that FR approaches zero when R does so, and that the maximal value of one coincides with the maximal value of the other.) The curves reveal that $\frac{\Delta\lambda}{\mu}$ increases with each additional berth; i.e., that added berths bring increasing returns to capacity.

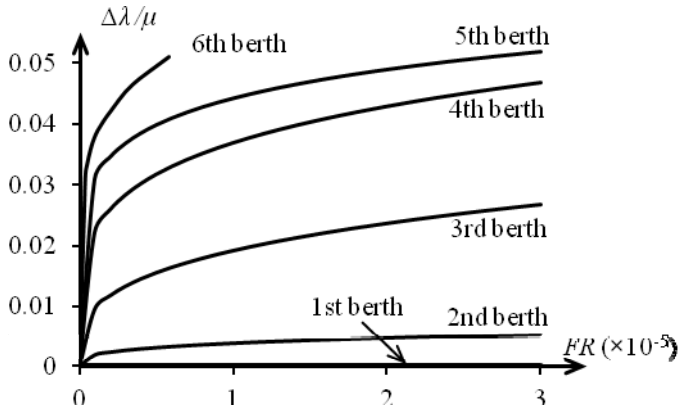

Figure 3 – Increasing returns to capacity caused by berth pooling effect

Although R and FR might seldom approach zero in an urban setting, the finding calls into question what handbooks have to say on the subject; i.e. the implication that added berths bring decreasing returns to capacity does not hold in general. More interesting evidence in this regard comes next by studying the more general case when R is between 0 and its maximum.

4.2.3 General Case with Intermediate Values of R

We now use our simulation model (see again Appendix C) to explore bus-stop capacities for the range of R . Once again, bus arrivals are assumed to be Poisson, and service time gamma-distributed with $C_S = 0.6$.

The curves in Figure 4a display the $\frac{\Delta\lambda}{\mu}$ for the first through the sixth berth. These too are shown as functions of FR, our chosen service metric and proxy for R. The curves reveal how the countervailing effects of blocking and berth pooling produce mixed results in terms of the capacities returned by adding berths to a stop.

When FR is small (but not approaching zero), additional berths can produce increasing returns to capacity, thanks to the berth pooling effect. For example, the figure shows that when $FR \approx 0.1$, adding a second berth brings increasing returns. (Note that when $FR \approx 0.1$, the curve for the second berth lies above that for the first.) This favorable trend does not continue, however. Note, for example, now the curve for the third berth lies below that for the second when $FR \approx 0.1$.

Toward the other extreme (e.g. when $FR \approx 0.7$), the curves reveal that added berths produce diminishing returns to capacity. This is because the blocking effect tends to dominate.

These findings are logical in light of what was unveiled for the two limiting cases. Yet, our finding that returns to capacity vary with FR or R runs counter to the *HCM*'s suggestion in this regard; i.e. using a single set of numbers for "effective berths" evidently does not suffice for all operating environments.

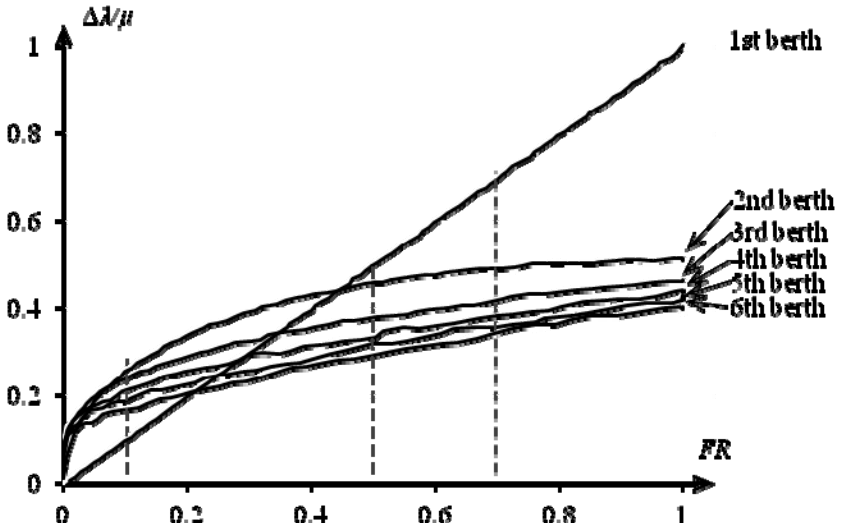

(a) Normalized incremental change in capacity versus FR

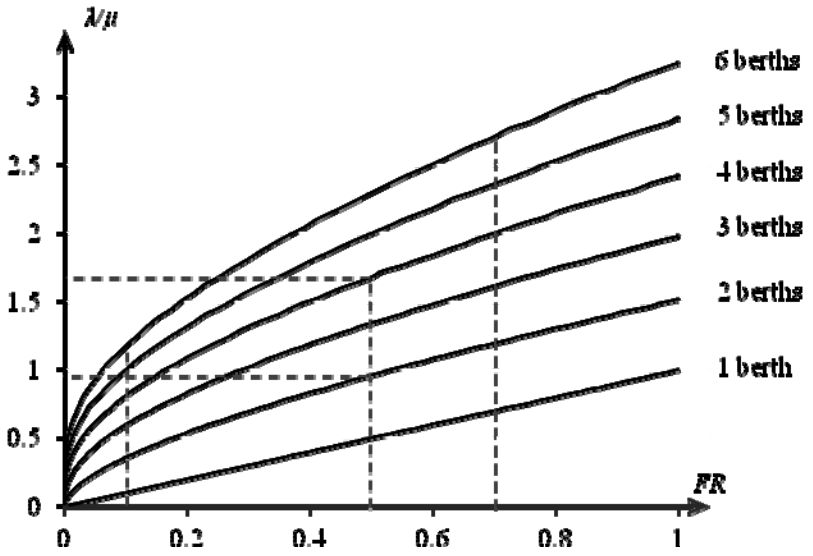

(b) Normalized capacity versus FR

Figure 4 – Normalized stop capacity and incremental change in capacity versus FR for multi-berth stops with Poisson bus arrivals and gamma-distributed service time ($C_S = 0.6$)

A graph like Figure 4a can be used in a number of practical pursuits. The same is true for variants, like the curves of FR versus normalized capacity ($\frac{\lambda}{\mu}$) shown in Figure 4b. More will be said on these matters in Section 5.

4.3 Variations in Service Time and Headway

Having explored the influences of FR and R , we now examine how the returns to capacity are influenced by the coefficients of variation in bus service time and bus headway. Simulation is again used to this end.

4.3.1 Bus Service Time

We continue to assume that bus arrivals are Poisson and that service time is gamma-distributed. Now, however, capacities will be explored for the range of $C_S \in [0, 1]$.

Figure 5a displays effects of C_S on the $\frac{\Delta\lambda}{\mu}$ for the first through the sixth berth when $FR = 0.15$. Note from the figure that increased returns to capacity come by adding a second berth to a stop (i.e., the curve for the second berth lies above that for the first). This is again thanks to the pooling effect at low FR . Further note that the curves for the second through the sixth berth exhibit downward slopes. This reveals an inverse influence of C_S on the returns to capacity. Additionally, the downward sloping curves for $c = 2 \sim 6$ in Figure 5b reveal how C_S exerts an inverse influence on stop capacity itself. These inverse influences become more dramatic as FR

increases. To illustrate, the above analysis is repeated, but for $FR = 1$. Results are displayed in Figure 6a and 6b.

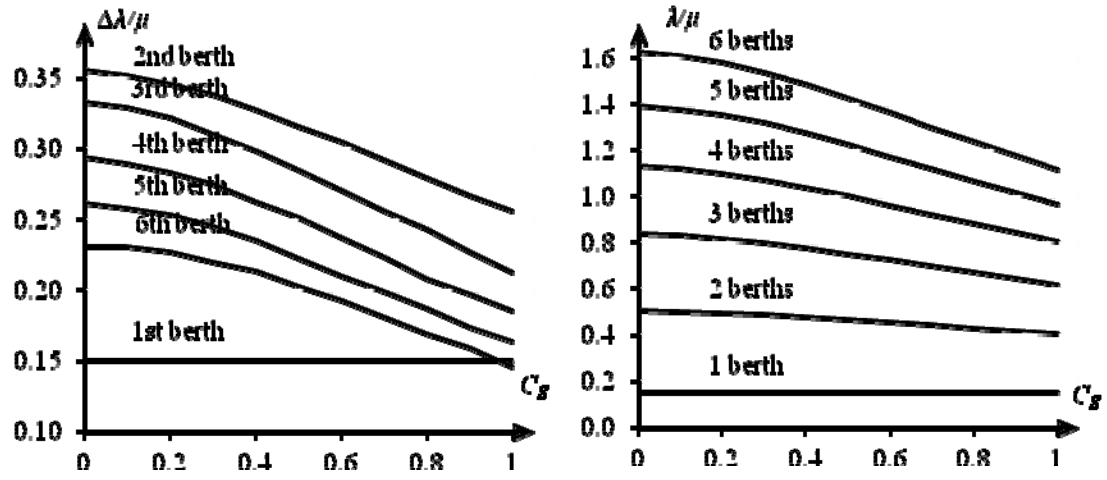

(a) Normalized incremental change in capacity versus C_S (b) Normalized capacity versus C_S

Figure 5 – Normalized capacity and incremental change in capacity versus C_S for multi-berth stops with $FR = 0.15$

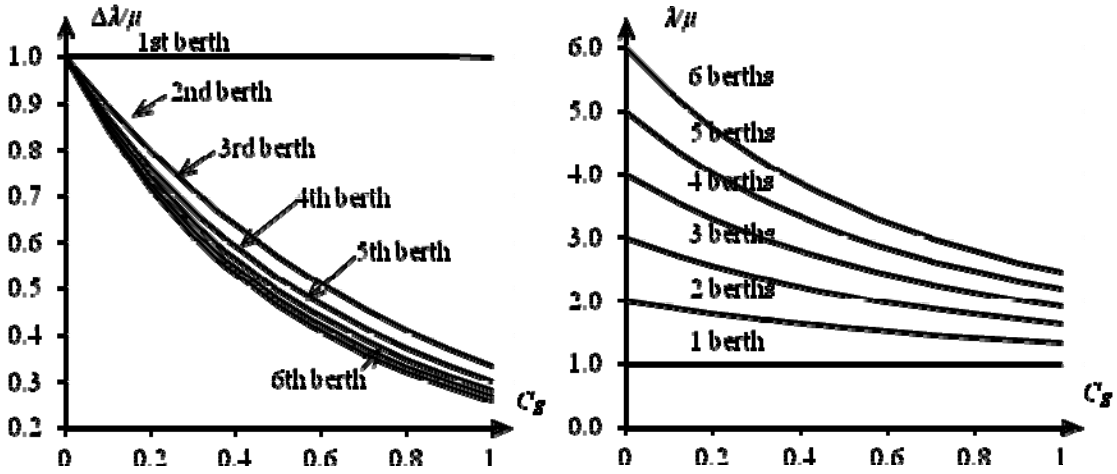

(a) Normalized incremental change in capacity versus C_S (b) Normalized capacity versus C_S

Figure 6 – Normalized capacity and incremental change in capacity versus C_S for multi-berth stops with $FR = 1$

4.3.2 Bus Headway

To explain how variations in bus arrival headway affect things, we will assume that: $FR = 0.15$; bus service time is gamma-distributed with $C_S = 0.6$; and bus headway is also gamma-distributed with a coefficient of variation, C_H , ranging from 0 to 1.

The curves in Figure 7a show that the first berth is relatively sensitive to C_H; i.e., the $\frac{\Delta\lambda}{\mu}$ diminishes precipitously with increasing C_H. As a result, the $\frac{\Delta\lambda}{\mu}$ for the second through even the sixth berth is greater than that achieved by the first berth when C_H is sufficiently high. For example, we see that adding a second berth to a stop produces increasing returns to capacity once C_H comfortably exceeds 0.6. Once again, however, we find that a stop's capacity for any c diminishes as C_H grows large; see Figure 7b. The above influences are found to disappear as FR approaches 1.

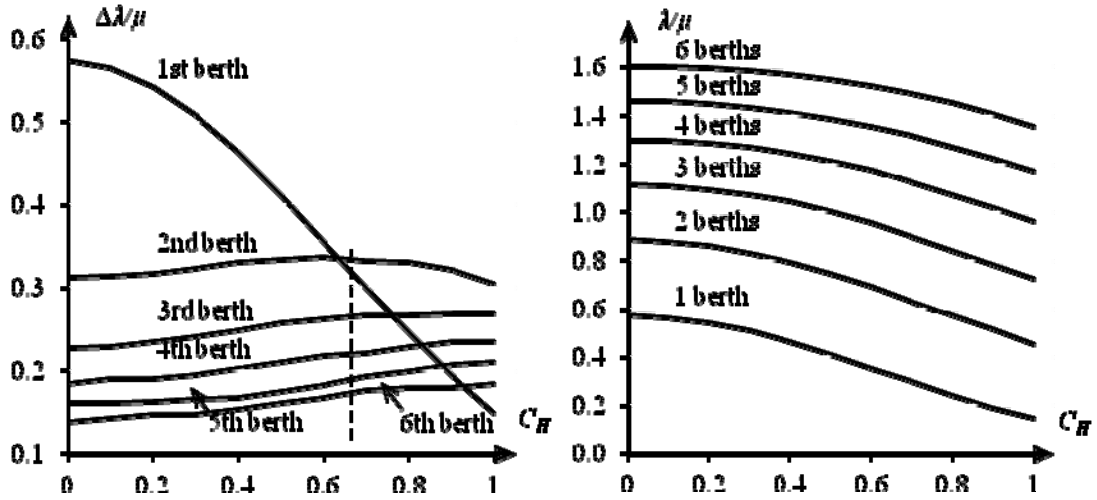

(a) Normalized incremental change in capacity versus C_H (b) Normalized capacity versus C_H

Figure 7 – Normalized capacity and incremental change in capacity versus C_H for multi-berth stops with $FR = 0.15$

5 Conclusions

The models presented in this paper account for key influences on the capacities of isolated, curbside bus stops. They do so in ways that are more complete than what has been offered by formulas in well-known handbooks. Through this more complete accounting come insights. The insights have practical implications.

For example, the models predict that variations in bus service time tend to diminish stop capacity, both for single- and multi-berth stops. (See Figures 1, 5b and 6b, and recall that an exception to this occurs when buses arrive at a single-berth stop as a Poisson process.) This finding speaks to the value of reducing service-time variations via the improved management of passenger boarding and alighting. Means of doing this might include the use of wider bus doors, improved loading platforms and off-board fare collection. Of course, these measures could also help reduce the average service time, and this too would favorably affect bus-stop capacity.

In contrast to formulas in professional handbooks, the present models also account for the effects of the bus arrival process at a stop. They predict that variations in bus headway can diminish stop capacity (Figure 7b), but can in some instances favorably affect the returns to capacity brought by a second through even a sixth berth relative to the returns from a single berth (Figure 7a). When the variation in headway is high and the FR is low, adding a second berth to a single-berth stop can bring increasing returns to capacity (Figures 4a and 7a). Knowledge of these cause and effect relations can be useful when choosing the number of berths to be deployed at a curbside stop.

To further illustrate the practical utility of our models, we ask the reader to refer again to Figure 4b. It displays relations between FR and normalized capacity for stops that range in size from 1 to 6 berths. Note how the curves in this figure can be used to determine the number of berths needed to achieve targets for FR and stop capacity. Or, they can be used to estimate FR given bus arrival rate and a specified number of berths. The figure can also help determine when it can be advantageous to split a single stop with many berths into multiple adjacent stops. For example, the reader can use Figure 4b to verify that, for a $FR = 0.5$, splitting a 4-berth stop into two 2-berth stops could increase capacity by nearly 15%. (That capacity is increased by splitting the stop is clearly evident in Figure 4a, since at $FR = 0.5$, the $\frac{\Delta\lambda}{\mu}$ for the third and fourth berths are lower than for the first and second berths.) Admittedly, this prediction assumes certain idealizations; e.g. that both the bus arrival processes and the service time distributions are comparable across the 2-berth stops; and that buses bound for one of these stops do not impede buses bound for the other.

To be sure, all of our present models are idealized, particularly since they apply to isolated stops. Yet in our view, these models represent a step toward better understanding bus-stop operation. Work is ongoing in regard to stops: that are not isolated, but are instead affected by traffic signals and other bus stops; that have limited space for storing bus queues; and that allow bus overtaking. In the mean time, one may still use our models to develop graphs that are similar to those shown here, but that are tailored to local conditions for target FR , variations in service time and headway, and so on.

Acknowledgement

Funding for this work was provided by the University of California Transportation Center and the Volvo Research and Educational Foundations.

Appendix A

Analytical Solution to a Single-Berth Stop with Uniform Bus Arrivals and Erlang-k Service Time (in Section 3.2)

Here we furnish a solution by applying a more general result given by Gross, et al. (2008) for a queueing system with generalized-Erlang distributed headways and service time ($\frac{GE_j}{GE_k/1}$, where GE_j and GE_k are the distributions of bus headway and bus service time, respectively)[8]. This general result is:

$$\overline{W_q}(s) = \frac{\prod_{m=1}^{k}\left[\left(-\frac{s_m}{\mu_m}\right)(s+\mu_m)\right]}{s\prod_{m=1}^{k}(s-s_m)}, \quad \text{(A.1)}$$

where $\overline{W_q}(s)$ is the Laplace-Stieltjes transform of the cumulative distribution function (CDF) of bus waiting time; $\mu_m\ (m=1,\dots,k)$ is the rate of the m -th exponential component of the GE_k distribution; and $s_m\ (m=1,\dots,k)$ is the m -th complex root with negative real parts of the following equation with argument s :

$$\prod_{m=1}^{j}\lambda_m\prod_{m=1}^{k}\mu_m - \prod_{m=1}^{j}[(\lambda]_m - s)\prod_{m=1}^{k}(\mu_m+s) = 0 \quad . \quad \text{(A.2)}$$

Equation (A.2) is also given in Gross, et al. (2008). The $\lambda_m\ (m=1,\dots,j)$ is the rate of the m -th exponential components of the GE_j distribution.

Since the means of the headway and the service time are $\sum_{m=1}^{j}\frac{1}{\lambda_m}$ and $\sum_{m=1}^{k}\frac{1}{\mu_m}$, respectively, we set $\lambda_m(m=1,\dots,j)=j\lambda$, $\mu_m(m=1,\dots,k)=k\mu=k$ so that the bus headway and the service time are Erlang-j and Erlang-k distributed, respectively; and so that the bus arrival rate and the service rate are λ and $\mu=1$, respectively. Given that when j approaches infinity, the limit of the Erlang-j distribution is a deterministic value, we let $j\to\infty$, so that the headway becomes constant. Then (A.2) becomes $\left(\frac{k}{k+s}\right)^k = e^{-\frac{s}{\lambda}}$.

[8] A generalized Erlang distribution is the convolution of independent but not necessarily identical exponential random variables. Here a bus headway can be expressed as the sum of j exponential components that are independent but may not be identical; and a bus service time can be expressed as the sum of k such components.

Let $R = \frac{\lambda}{\mu} = \lambda$, such that the solution of the above equation is:

$$s_m = -kR \cdot \text{LambertW}\left(-\frac{1}{R} e^{-\frac{1}{R} - \frac{2\pi(m-1)i}{k}}\right) - 1, (m = 1, \dots, k),$$

(A.3)

where function $\text{LambertW}(\cdot)$ is the inverse function of $f(w) = we^w$, which is multi-valued in the field of complex numbers, and has no closed-form expression; and i is the imaginary unit.

By picking up the roots of s_m's with negative real parts, plugging them into (A.1), and then taking a partial-fraction expansion, we obtain:

$$W_q(s) = \frac{\prod_{m=1}^{k}\left[(-s_m)\left(\frac{s}{k}+1\right)\right]}{s\prod_{m=1}^{k}(s-s_m)} = \frac{1}{s} - \sum_{m=1}^{k}\frac{\beta_m}{s-s_m},$$

(A.4)

where β_m are constant coefficients to be determined by:

$$\beta_m = \prod_{n=1, n\neq m}^{k}\left(\frac{-s_n}{s_m - s_n}\right)\left(\frac{s_m}{k}+1\right)^k. \quad (A.5)$$

By applying the inverse Laplace transform on (A.4), we obtain the CDF of the bus waiting time:

$$W_q(t) = 1 - \sum_{m=1}^{k}\beta_m e^{s_m t}.$$

Therefore the failure rate becomes $FR = 1 - W_q(0) = \sum_{m=1}^{k}\beta_m$. (A.6)

For any given $k = c_s^{-2}$, the last term of (A.6) is a function of $R = \frac{\lambda}{\mu}$. Thus we find the relation between FR and $\frac{\lambda}{\mu}$. The results can be obtained numerically.

Appendix B

Derivation of Equation (4) in Section 4.2.1

For a fixed number of berths, c, let $T(c) = \max_{i}(\bar{S}_i, (i = 1,2,\dots,c))$ be the platoon service time, where $\bar{S}_i$ is the service time of the i-th bus in the platoon. All $\bar{S}_i$'s are independent, identically distributed random variables subject to the CDF of $F_S(t)$. Let $F_{T(c)}(t)$ be the CDF of $T(c)$. Thus we have:

$$F_{T(c)}(t) = P\{T(c) \leq t\} = P\{\bar{S}_i \leq t, i = 1,2,\dots,c\}$$

$$= \prod_{j=1}^{c} P\{S_j \le t\}$$

$$= \prod_{j=1}^{c} F_S(t) = (F_S(t))^c .$$

From the identity $E[T(c)] = \int_{t=0}^{\infty} (1 - F_{T(c)}(t))dt$, we have:

$$E[T(c)] = \int_{t=0}^{\infty} (1 - (F_S(t))^c)dt .$$

Appendix C

Simulation Algorithm for the Multi-Berth Stops Analyzed in Sections 4.2 and 4.3

First we introduce the following notation used in our simulation model:

H_i – Headway (in minutes) between the arrivals of Bus_{i-1} and Bus_i, and H_1 is the system idle time before the first bus arrives;

S_i – Service time (in minutes) of Bus_i, not including the time that Bus_i waits to depart the stop after it has finished serving passengers;

P_i – The position (number) of the berth where Bus_i dwells to serve passengers; where berths are numbered $1, 2, \ldots, c$ from the downstream to the upstream berth;

$W_{i,q}$ – Waiting time in the queue (in minutes) of Bus_i before it enters the stop;

$W_{i,b}$ – Waiting time in the berth (in minutes) of Bus_i after its service is finished; and

F_i – Indicator that takes 1 if Bus_i fails to enter the berth immediately upon its arrival to the stop, and 0 otherwise.

The dynamic equations describing our simulation model are:

For each $i = 1, 2, \ldots,$

$$W_{i+1,q} = \begin{cases} \max\{0, W_{i,q} + S_i + W_{i,b} - H_{i+1}\}, & \text{if } P_i = c \\ \max\{0, W_{i,q} - H_{i+1}\} & \text{otherwise;} \end{cases}$$

$$P_{i+1} = \begin{cases} 1, & \text{if } W_{i,q} + S_i + W_{i,b} - H_{i+1} - W_{i+1,q} \le 0 \\ P_i + 1, & \text{otherwise;} \end{cases}$$

$$W_{i+1,b} = \max\{0, W_{i,q} + S_i + W_{i,b} - H_{i+1} - W_{i+1,q} - S_{i+1}\};$$

$$F_{i+1} = \begin{cases} 1, \text{if } W_{i+1,q} > 0 \\ 0, \text{if } W_{i+1,q} = 0. \end{cases}$$

The H_i and S_i $(i = 1, 2, 3, \ldots)$ are inputs to the simulation. We assume that H_i follows a gamma distribution with mean $\frac{1}{\lambda}$ and coefficient of variation C_H. (For Poisson bus arrivals, $C_H = 1$ and H_i is exponentially distributed.) We further assume that S_i follows another gamma distribution with mean $\frac{1}{\mu} = 1$ and coefficient of variation C_S. The simulation starts from an initial state in which the stop is empty (i.e., $W_{1,q} = W_{1,b} = F_1 = 0$ and $P_1 = 1$) and ends at the same state to diminish stochastic error. The resulting performance measure PR is obtained by averaging the F_i.

References

Danas, A., 1980. Arrivals of passengers and buses at two London bus stops. *Traffic Engineering and Control*, 21(10), 472-475.

Fernandez, R., 2001. A new approach to bus stop modeling. *Traffic Engineering and Control*, 42(7), 240-246.

Fernandez, R. and Planzer, R., 2002. On the capacity of bus transit systems. *Transport Reviews*, 22(3), 267-293.

Gardner, G., Cornwell, P. R., and Cracknell, J. A., 1991. *The Performance of Busway Transit in Developing Cities*. TRRL Research Report 329, Transport and Road Research Laboratory, Crowthorne.

Ge, H., 2006. *Traffic impacts of bus stops in urban area and related optimization techniques* (translated from Chinese). PhD Thesis, Southeast University, China.

Gibson, J., Baeza, I., and Willumsen, L. G., 1989. Bus stops, congestion, and congested bus stops. *Traffic Engineering and Control*, 30(6), 291-302.

Gross, D., Shortle, J. F., Thompson, J. M., and Harris, C. M., 2008. *Fundamentals of Queueing Theory*, 4th Ed. John Wiley & Sons, Inc., Hoboken, New Jersey.

ITE, 1999. *Transportation Planning Handbook*. Institute of Transportation Engineers, New Jersey.

Kohler, U., 1991. Capacity of transit lanes. *Proceedings of the International Symposium on Highway Capacity*, Karlsruhe, Germany.

St. Jacques, K. R. and Levinson, H. S., 1997. *Operational Analysis of Bus Lanes on Arterials*. TCRP Report 26, Transportation Research Board, National Research Council, Washington D.C.

Szász, P. A., Montana, L. de C., and Ferreira, E. O., 1978. *COMONOR: ordinated bus convoy*. Technical Paper 9, Companhia de Engenharia de Trafego, Sao Paulo.

TRB, 1985. *Highway Capacity Manual*. Transportation Research Board, National Research Council, Washington D.C.

TRB, 2000. *Highway Capacity Manual*. Transportation Research Board, National Research Council, Washington D.C.

TRB, 2003. *Transit Capacity and Quality of Service Manual*, 2nd Ed. Transportation Research Board, National Research Council, Washington D.C.